Direct Study of the Proximity Effect in the Normal Layer inside of the Stacked SINIS Device

I. P. Nevirkovets and O. Chernyashevskyy

Department of Physics and Astronomy, Northwestern University, Evanston, Illinois 60208, USA
Institute for Metal Physics, NASU, 03680 Kyïv, Ukraine

J. B. Ketterson

Department of Physics and Astronomy, Department of Electrical and Computer Engineering, and Materials Research Center, Northwestern University, Evanston, Illinois 60208, USA

(Received 6 June 2005; published 8 December 2005)

We have observed a striking anisotropy in the electrical transport of layered multiterminal SINIS structures [where S, I, and N denote a superconductor (Nb), an insulator (AlO_x), and a normal metal (Al), respectively]. We find that the lateral conductivity of the N layer is dissipative, but a superconducting current can flow normal to the structure, suggesting a direct Josephson coupling between the external S electrodes. A small coherent contribution to the lateral conductivity of the N layer is observed near zero voltage.

DOI: 10.1103/PhysRevLett.95.247008 PACS numbers: 74.45.+c, 74.50.+r, 74.78.Fk, 85.25.Am

Over the past few decades, the proximity effect has attracted sustained interest [1–6]. In recent years, it has been recognized that, on the microscopic level, the proximity effect may be described in terms of Andreev reflections [7]. In spite of this progress, important questions remain. In sandwich-type structures, the electronic spectrum of the normal metal is inferred indirectly from the characteristics of the entire system, measured perpendicular to the layers, but clearly, additional information on the state of the N layer could be obtained if the lateral electrical transport characteristics were measured.

Earlier, Capogna and Blamire reported observations of the proximity effect through high-conductance tunnel barriers in SINIS junctions [8], based on the appearance of a Josephson current above the superconducting transition temperature, T_c^*, of the N layer (here S, I, and N denote a superconductor, an insulator, and a normal metal, respectively). However, the two-terminal SINIS configuration [8] does not allow one to directly measure conductivity of the N film in lateral direction and thereby establish whether its superconducting properties are isotropic or anisotropic.

Well before these experiments, a similar temperature dependence (with a characteristic "tail" above T_c^*) was observed for a coherent current in SIN junctions in a study of fluctuation superconductivity [9]. It was predicted that the order parameter of the S electrode can couple to a fluctuating order parameter in the N electrode, thereby giving rise to a pair current through the barrier in excess of the usual quasiparticle current [10–12]. Recently, a phenomenological model of SINIS junctions was developed [13]; in this work, a coherent current in a SIN junction [9–12] was treated in terms of the proximity effect.

It is clear from the above discussion that the nature of the Josephson current in SINIS junctions above T_c^*, as well as the actual state of the N layer (superconducting or not?), requires further clarification. Furthermore, since the experiments [9,14] were carried out using low-transparency junctions, a study of the proximity effect through a high-transparency barrier in a NIS junction should be of general interest.

Here we present results of an experimental study of the *lateral* characteristics of the N layer in multiterminal sandwich-type SINIS and NIS devices where the specific tunneling resistance of the tunnel barriers is of the order of $1 \times 10^{-7}\ \Omega\,\mathrm{cm}^2$. Our multilayer SINIS ($Nb/Al/AlO_x/Al/AlO_x/Al/Nb$) structures were *in situ* fabricated using a standard procedure described elsewhere [15]. A schematic cross-sectional view of the multiterminal SINIS device is shown in Fig. 1(a). Here we describe devices with a width $W = 10\ \mu$m and lengths $L_b = 19\ \mu$m and $L_t = 11\ \mu$m for the bottom and top junctions, respectively. The 150 nm-thick Al layer facilitates a *nonsuperconducting* electrical contact to the N layer; to suppress the parasitic proximity effect between this Al layer and the topmost Nb layer (used to minimize the contribution of the normal leads to the conductivity), 21–40 nm of Zr was deposited between Nb and Al. Such contacts were also used in measurements on NIS junctions [Fig. 1(b)], fabricated on the same chip as the SINIS devices, to determine the influence of the top Nb layer on the lateral conductivity of the Al electrode.

First, we consider the current-voltage characteristics (CVC) for a typical SINIS device with a thickness of the

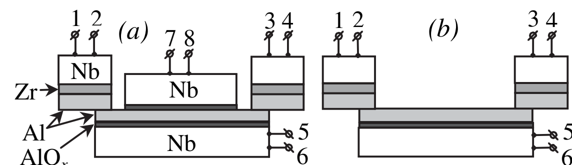

FIG. 1. Schematic cross-sectional view of the structures studied.

 © 2005 The American Physical Society

Al middle layer $d_{\rm Al} = 13$ nm (referred to as device 1) measured at 1.8 K (see Fig. 2). Curve 1 is for the top junction (using 3 and 8 as current and 2 and 7 as voltage terminals), while curve 2 is for the bottom junction (using 3 and 6 as current and as 2 and 5 voltage terminals). Curve 3 shows the CVC of the N layer, measured between the terminals 1 and 4 (for current) and 2 and 3 (for voltage); curves 4–6 were measured using the terminals 5 and 7 for current and the terminals 2 and 8, 6 and 2, and 6 and 8 for voltage (corresponding to the top and bottom junctions, and to the entire SINIS multilayer, respectively). As can be seen from curves 1 and 2 in Fig. 2, the top NIS and bottom SIN junctions, when measured separately, have different apparent critical currents, $I_{\rm ct}$ and $I_{\rm cb}$, such that $I_{\rm ct} > I_{\rm cw} > I_{\rm cb}$, where $I_{\rm cw}$ is the critical current of the whole structure (cf. curve 6); the respective $I_{\rm c}$ levels are marked by arrows. However, when feeding the current through terminals 5 and 7, we find that for the same junctions the critical currents $I'_{\rm ct}$ and $I'_{\rm cb}$ (cf. curves 4,5) are identical to $I_{\rm cw}$. The critical current vs magnetic field dependences $I_{\rm ct}(H)$, $I_{\rm cw}(H)$, and $I_{\rm cb}(H)$ were measured to demonstrate good junction quality for all the junctions contained in the multiterminal device (see the left inset of Fig. 2, curves 1–3, respectively). The $I_{\rm cw}(H)$ dependence for the entire device closely follows that for an ideal Josephson junction.

Identical values for $I'_{\rm ct}$, $I'_{\rm cb}$, and $I_{\rm cw}$ can be due to either inductive coupling (observed earlier in SIS stacks [16]) or direct Josephson coupling between the external S electrodes. In the case of a SIS$'$IS stack, even with a very thin S$'$ layer, it is possible to drive one junction into the resistive state and measure the $I_{\rm c}(H)$ dependence of the other junction, which then displays an increased period of the diffraction pattern [16]. However, in our SINIS multiterminal devices, it was not possible to set one junction into the resistive state while keeping the other in the superconducting state. Even if we current bias the top and bottom junctions independently, so that there is a voltage across one (the top) junction, while trying to achieve a region of dc Josephson current in the second (bottom) junction, the system adjusts itself in such a manner that the voltage between the two barriers becomes zero. This results in a nonequilibrium state of the device, in which the apparent value of $I_{\rm cb}$ is enhanced up to the $I_{\rm ct}$ value. These observations, along with the condition that the thickness of the N (Al) layer is less than an electron mean free path (estimated to be above 20 nm from resistance measurements of similar reference Al films), suggest a direct Josephson coupling between the S electrodes. The fact that it is not possible to measure a true value of $I_{\rm c}$ of one junction independent of the state of the other suggests that the order parameter in the middle N layer is not independently capable of achieving a global phase.

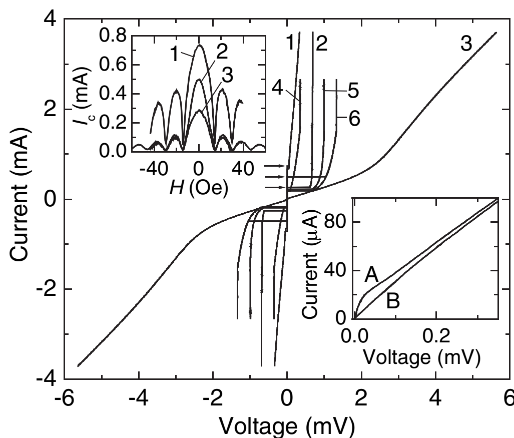

FIG. 2. CVC of a multiterminal SINIS device at 1.8 K. Curves 1–6 are recorded using the following terminals for current (voltage) [cf. Fig. 1(a)]: 3 and 8 (2 and 7); 3 and 6 (2 and 5); 1 and 4 (2 and 3); 5 and 7 (2 and 8); 5 and 7 (6 and 2); 5 and 7 (6 and 8). Left inset shows $I_{\rm c}$ vs H dependences for the top junction, the structure as a whole, and the bottom junction (curves 1–3, respectively); cf. respective CVC 1, 2, and 6 in the main panel. Right inset: initial portion of curve 3 for $H = 0$ (curve A) and for $H = 30$ Oe (curve B).

We now focus on the properties of the N layer (see curve 3 in Fig. 2). The right inset of Fig. 2 shows an initial portion of curve 3 on a magnified scale for $H = 0$ (curve A) and for an in-plane magnetic field of 30 Oe (curve B). These curves display three important features: (1) The lateral conductivity of the Al layer is *dissipative*. This is a counterintuitive result given the fact that a considerable Josephson current (about 500 μA) can flow through the film in the vertical direction (at 1.8 K). (2) There is a small contribution to the current near zero voltage that can be completely suppressed in a small magnetic field. This *coherent* contribution resembles a current observed earlier on low-transparent SIN junctions and interpreted as a manifestation of fluctuation superconductivity in the N electrode [9]. (3) There is a nonlinearity in the CVC at a voltage $V \approx 2\Delta_{\rm Nb}/e$, where $\Delta_{\rm Nb}$ is the Nb superconducting energy gap. This feature may be explained as follows: a fraction of the electrons entering the N layer leaks into S, and then reenters the N layer. As a simplified model, we envision two NISIN junctions connected in parallel to the N layer; the nonlinearity in the CVC of these junctions results in the respective feature in the CVC of the N layer.

Before analyzing the CVC of the Al layer near $V = 0$ in more detail, we discuss how the specific geometry of our samples may influence the shape of the CVC. In order to determine the contribution of the Al/Zr/Nb terminals to the conductivity of the Al layer, we deposited 8–18 nm-thick Al films onto oxidized Si substrates under conditions identical to those that we used to deposit Al layers in our SINIS devices. One part of the film was processed to have a configuration identical to that of the bottom junction (cf. Fig. 1); the Al/Zr/Nb contact leads were formed identically to those in our SINIS devices. Standard 4-terminal R vs T measurements were performed on the other part of the same Al film, which had much larger lateral dimensions. Comparing the $R(T)$ data for the two parts of the film, we concluded that the contribution of the Al/Zr/Nb contact

leads to the resistance of the 18 nm-thick Al layer being below 5%; we will neglect this contribution. From these measurements, we also established that an Al film with Al/Zr/Nb contacts is not superconducting and displays a linear CVC down to 1.8 K (the lowest temperature available in that experiment); therefore, the nonlinearity seen in curve 3 (cf. Fig. 2) is due to the influence of the superconducting Nb electrodes, i.e., due to the proximity effect *through* the tunnel barriers.

Since portions of the middle Al layer in our devices are not covered by the top Nb electrode [see Fig. 1(a)], it is important to know how this affects the conductivity of the Al. To examine how the CVC of the Al layer is modified if the top Nb electrode is *missing*, in addition to an ordinary SINIS device [cf. Fig. 1(a)], a device was fabricated on the same chip with the top Nb layer etched away [see the structure in Fig. 1(b)]. The respective multilayered structures were deposited in a run different from that used to fabricate device 1; we will refer to the devices resulting from the second run as type 2 devices. In these devices, the oxidation conditions for the top and bottom junctions were nominally identical; the specific tunneling resistance of the double-barrier junction as a whole was about $3 \times 10^{-7}\ \Omega\,\mathrm{cm}^2$, and d_{Al} was in the range of 8–18 nm. Here we consider in more detail the characteristics of devices with $d_{\mathrm{Al}} = 18$ nm; the devices with other values of d_{Al} displayed qualitatively the same properties.

Figure 3(a) shows the CVC of the SIN junction recorded with the current fed between terminals 1 and 5, and the voltage measured between terminals 2 and 6 (curves 1 and 2), along with that for the Al layer of the same junction (curves 3 and 4), and for the Al layer of the related SINIS junction on the same substrate (curves 5 and 6); the last two data sets were measured using the current terminals 1 and 4 and the voltage terminals 2 and 3 (cf. Fig. 1). Curves 1, 3, and 5 were recorded in zero magnetic field; curves 2 and 4 are for a parallel field of 20 Oe, and curve 6 is for 14 Oe. Curves 1–4 were measured at 1.9 K and curves 5,6 were measured at 2.2 K. We observe that curves 1,2 display a gap feature at $V \approx \Delta_{\mathrm{Nb}}/e$, as expected for a Nb-I-Al SIN junction, whereas the curves 3,4 display a gap feature at $V \approx 2\Delta_{\mathrm{Nb}}/e$ (similarly to the curve 3 in Fig. 2). We did not observe any indication of an Al energy gap in these curves (with 1 μV resolution).

The initial portions of these curves are shown on a magnified scale in the inset of Fig. 3(a). In the SIN case (curves 1–4), we see that both the conductivity across the barrier (curves 1,2) and the conductivity of the N layer (curves 3,4) have a small coherent contribution near zero voltage. Moreover, curve 3 looks like a tilted version of curve 1; if we subtract a linear background with a resistance of about 2.3 Ω from curve 3, we obtain a characteristic [curve B in Fig. 3(b)] that coincides with that of the SIN junction [curve A in Fig. 3(b)] near $V = 0$. Therefore, the coherent contribution in the conductivity of the N layer may originate from the coherent current flowing through the barrier(s), and the magnitude of this current can be inferred from the response of the N layer. In comparison with the CVC of the N layer of the SIN junction (curve 3), the characteristic of the N layer of the SINIS junction (curve 5) displays a higher conductivity and a higher (at the same temperature), but qualitatively very similar, coherent current, because of an influence of the top Nb electrode. This experiment indicates the following: (1) the CVC of the N film in a SINIS device and in the related SIN junction are similar, so that in spite of the fact that a portion of the N layer of our SINIS device is not covered by the top S electrode, the conductivity of this layer qualitatively displays the behavior it has inside of the device; (2) assuming that the small coherent current in the CVC of the N layer is due to the proximity effect (interpreted as injection of the superconducting electrons from S to N through a tunnel barrier), this effect is unlikely to be responsible for the much larger supercurrent that can flow perpendicular to the entire multilayer device.

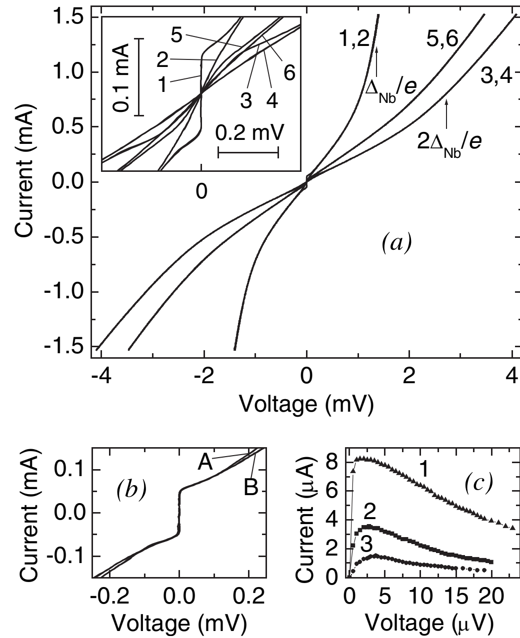

FIG. 3. (a) CVC of the SIN junction (curves 1,2) and of the N electrode of the same junction (curves 3,4) at 1.9 K (curves 1,3 are recorded for $H = 0$; curves 2,4 are recorded for $H = 20$ Oe); CVC of the N layer of the SINIS junction at 2.2 K: curve 5 is recorded for $H = 0$; curve 6 is measured for $H = 14$ Oe. The inset shows initial portions of these curves on a magnified scale. (b) CVC of the initial portion of the SIN junction at 1.9 K (curve A) along with the CVC of the N electrode of the same junction corrected by subtracting the voltage contribution from a constant resistance of 2.3 Ω (curve B). (c) Coherent current vs voltage dependence for the CVC of the SIN junction at 2.6, 2.94, and 3.34 K (curves 1–3, respectively).

To better understand the nature of this proximity effect, we next consider the temperature dependences of the maximum supercurrent, $I_{\mathrm{cw}}(T)$, through the SINIS device, and the maximum coherent current, $I_{\mathrm{m}}(T)$, through the related SIN junction. These data are plotted in Fig. 4 [squares for $I_{\mathrm{cw}}(T)$ and circles for $I_{\mathrm{m}}(T)$]. Note that the

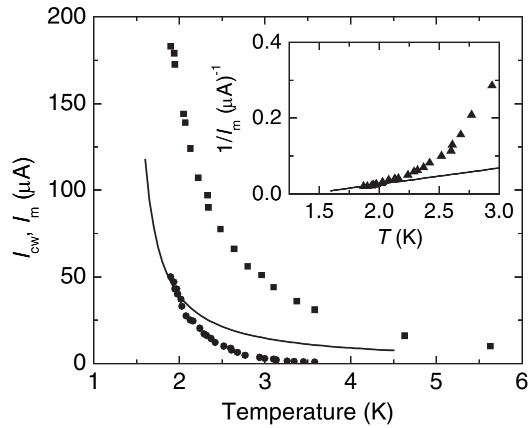

FIG. 4. Temperature dependence of the Josephson current measured across the layers in a SINIS device (squares) and the related SIN junction (circles). Solid line is the theoretical $I_m(T)$ dependence for the SIN junction according to Ref. [9]. Inset: experimental (scattered data) and theoretical [9] (solid line) $I_m^{-1}(T)$ dependence.

current I_{cw} is considerably higher than I_m. The difference is more apparent for devices with thinner Al interlayers. Here the magnitude of I_m is of the same order as that for devices with larger d_{Al}; however, the magnitude of I_{cw} increases dramatically. For devices with $d_{Al} = 18$ nm, the ratio I_{cw}/I_m is 3.6 at 1.9 K (cf. Fig. 4), whereas for devices with $d_{Al} = 8$ nm, $I_{cw} = 2.2$ mA, and $I_m = 80$ μA (at 1.9 K), yielding $I_{cw}/I_m = 27.5$. This is in disagreement with a phenomenological model [13], according to which $j_m = j_{cw}/2$ (here j_m, j_{cw} are the densities of the respective currents I_m, I_{cw}). Obviously the presence of the top S layer does not simply double the Josephson energy of the whole double-barrier system, but changes the system qualitatively. The above experimental fact is consistent with the idea that the Josephson tunneling through the two barriers in our SINIS devices is *coherent*. This conclusion is in disagreement with the theory by Kupriyanov *et al.* and Brinkman and Golubov [17,18], according to which the supercurrent in a SINIS junction is governed by a single parameter $\gamma_{eff} = (2d_{Al}/D)(2\pi T_c/\hbar v_F)$, where D is the transparency of a single barrier (with both barriers assumed to have equal transparency), T_c is the critical temperature of S, and v_F is the Fermi velocity in N. The coherent regime takes place if $\gamma_{eff} < 1$ and breaks down at $\gamma_{eff} \gg 1$. Estimation of γ_{eff} using parameters from our experiment ($D \simeq 0.73 \times 10^{-4}$, $T_c = 9$ K, and $v_F = 1.3 \times 10^8$ cm/s [19]) yields $\gamma_{eff} \simeq 2800$, implying that, according to the model mentioned above, the tunneling is incoherent.

Finally, we compare our experimental data on $I_m(T)$ (circles in Fig. 4) with the theory based on superconducting fluctuations [9–12]. The solid line in Fig. 4 shows $I_m(T)$ predicted by expression (27) from Ref. [9] with $T_c^* = 1.4$ K and a critical magnetic field $H_c = 300$ Oe (used as a fitting parameter). Here we used the experimental value $T_c^* = 1.4$ K, measured (in a separate experiment) on the 18 nm-thick electrode of the SIN junction [cf. Fig. 1(b)], and on an 18 nm-thick Al film deposited under the same conditions for reference. According to the theory [9], the dependence $I_m^{-1}(T)$ is linear near T_c^*, crossing the T axis at T_c^*. In the inset of Fig. 4 we have plotted both experimental (points) and theoretical (solid line) $I_m^{-1}(T)$ dependences, which are in agreement with each other at lower temperatures.

However, the voltage V_m, associated with the current I_m, is considerably lower than that predicted by the theory [9,13]. From the data sets 1, 2, and 3, shown in Fig. 3(c), we obtain $V_m = 2$, 3, and 4 mV at temperatures of 2.6, 2.94, and 3.34 K, respectively; on the other hand, the theory predicts values in the range 130–210 mV. This discrepancy observed on devices with relatively high-transparency barriers may be due to a combination of superconducting fluctuations in the Al and a traditional proximity effect through the barriers.

We are thankful to E. Goldobin for letting us use his GOLDEXI software. This work was supported by the National Science Foundation under the Grant No. EIA-0218652 and use was made of facilities operated by the NSF-supported Materials Research Center.

[1] H. Meissner, Phys. Rev. **109**, 686 (1958).
[2] P. G. de Gennes and D. Saint-James, Phys. Lett. **4**, 151 (1963).
[3] W. L. McMillan, Phys. Rev. **175**, 559 (1968).
[4] E. L. Wolf and G. B. Arnold, Phys. Rep. **91**, 31 (1982).
[5] W. L. McMillan, Phys. Rev. **175**, 537 (1968).
[6] B. Pannetier and H. Courtois, J. Low Temp. Phys. **118**, 599 (2000).
[7] A. F. Andreev, Sov. Phys. JETP **19**, 1228 (1964).
[8] L. Capogna and M. G. Blamire, Phys. Rev. B **53**, 5683 (1996).
[9] J. T. Anderson, R. V. Carlson, and A. M. Goldman, J. Low Temp. Phys. **8**, 29 (1972).
[10] L. G. Aslamazov and A. I. Larkin, Phys. Lett. **26A**, 238 (1968).
[11] R. A. Ferrell, J. Low Temp. Phys. **1**, 423 (1969).
[12] D. J. Scalapino, Phys. Rev. Lett. **24**, 1052 (1970).
[13] A. M. Kadin, Supercond. Sci. Technol. **14**, 276 (2001).
[14] K. Yoshihiro and K. Kajimura, Phys. Lett. **32A**, 71 (1970).
[15] I. P. Nevirkovets, O. Chernyashevskyy, J. B. Ketterson, and E. Goldobin, J. Appl. Phys. **97**, 123903 (2005).
[16] I. P. Nevirkovets, J. E. Evetts, and M. G. Blamire, Phys. Lett. A **187**, 119 (1994).
[17] M. Yu. Kupriyanov, A. Brinkman, A. A. Golubov, M. Siegel, and H. Rogalla, Physica (Amsterdam) **326C–327C**, 16 (1999).
[18] A. Brinkman and A. A. Golubov, Phys. Rev. B **61**, 11 297 (2000).
[19] P. Santhanam and D. E. Prober, Phys. Rev. B **29**, R3733 (1984).